Communication



# Shining a New Light on the Classical Concepts of Carbon-Isotope Dendrochronology

Thomas Wieloch *

Posted Date: 1 March 2024

doi: 10.20944/preprints202403.0014.v1

Keywords: carbon stable isotopes, climate reconstruction, intramolecular isotope analysis, plant-environment interactions, tree rings, variance component analysis, water-use efficiency, whole-molecule isotope analysis

 doi:10.20944/preprints202403.0014.v1



*Perspective*

# Shining a New Light on the Classical Concepts of Carbon-Isotope Dendrochronology

**Thomas Wieloch**[1,2,*]

[1] Department of Forest Genetics and Plant Physiology, Swedish University of Agricultural Sciences, Umeå Plant Science Centre, 90183 Umeå, Sweden
[2] Division of Geological and Planetary Sciences, California Institute of Technology, 91125 Pasadena, USA
* Correspondence: thomas.wieloch@slu.se

**Abstract:** Retrospective information about the climate system and plant ecophysiology are key inputs in climate and Earth system modelling. Dendrochronology provides such information with large spatiotemporal coverage, and stable carbon isotope ($^{13}C/^{12}C$) analysis across tree-ring series is among the most advanced dendrochronological tools. For the past seventy years, this analysis was performed on whole molecules, and, to this day, $^{13}C/^{12}C$ variation is attributed to $^{13}C$ discrimination during $CO_2$ diffusion into leaves and assimilation by rubisco. By contrast, $^{13}C$ discrimination by post-rubisco processes is presumed constant. Here, recently reported results on the first dataset of intramolecular $^{13}C$ discrimination in tree rings were synthesised by variance component analysis. The emerging picture is not consistent with the classical (DR-discrimination-centred) concepts and practices of carbon-isotope dendrochronology. Specifically, leaf and stem post-rubisco discrimination each account for more variation in the data than diffusion-rubisco discrimination, i.e., post-rubisco discrimination is not constant. Furthermore, diffusion-rubisco discrimination is used widely as proxy of leaf intrinsic water-use efficiency (*iWUE*), a key determinant in the responses of global biogeochemical cycles to climate change. However, since diffusion-rubisco discrimination is a small component of the total data variance, whole-molecule analysis yields confounded *iWUE* estimates, yet intramolecular analysis will likely offer solutions. Lastly, all currently observed $^{13}C/^{12}C$-climate relationships are attributed to diffusion-rubisco discrimination. However, here, relationships with temperature and radiation derive from leaf-level post-rubisco discrimination while relationships with precipitation derive from stem-level post-rubisco discrimination. That said, advances in mass spectrometry may soon make intramolecular $^{13}C/^{12}C$ analysis broadly available taking carbon-isotope dendrochronology to the next level.

**Keywords:** carbon stable isotopes; climate reconstruction; intramolecular isotope analysis; plant-environment interactions; tree rings; variance component analysis; water-use efficiency; whole-molecule isotope analysis

## Introduction

Tree rings are natural archives containing encoded information about plant-environment interactions and the climate of the past. This information is (to a large extent) inaccessible to manipulation and monitoring experiments, and dendrochronologists are striving to decipher it to contribute to a better understanding of the climate system, regional and global biogeochemical cycles, and plant functioning. Stable carbon isotope ($^{12}C$, $^{13}C$) analysis across tree-ring series is among the most advanced dendrochronological tools available today. This tool has (*inter alia*) been used to reconstruct leaf intrinsic water-use efficiency ($CO_2$ uptake relative to $H_2O$ loss, *iWUE*), air temperature, solar radiation, air relative humidity, precipitation, and drought over past centuries at various locations worldwide (1–6).

Seventy years ago, tree-ring $^{13}C/^{12}C$ ratios were measured for the first time (7, 8). While early studies analysed whole-wood samples, most recent studies analyse cellulose, a glucose polymer

 doi:10.20944/preprints202403.0014.v1



extracted from tree rings to preclude error due to variation in wood composition (arguments given below apply to cellulose but not necessarily to wood) (6). Tree-ring cellulose $^{13}C/^{12}C$ data are commonly expressed in terms of $^{13}C$ discrimination, $\Delta_{trc}$, denoting carbon isotope changes caused by physiological processes (9). Current data interpretations invoke a simple mechanistic model accounting for $^{13}C$ discrimination accompanying two processes: $CO_2$ diffusion from ambient air into leaf intercellular air spaces (or chloroplasts) and carbon assimilation by rubisco (6, 10, 11), collectively termed diffusion-rubisco (DR) discrimination (12). Carbon assimilated by leaf phospho*enol*pyruvate carboxylase (PEPC) is thought to not enter cellulose biosynthesis or significantly affect its isotope composition (13).

Variation in DR discrimination depends on the ratio of intercellular-to-ambient $CO_2$ concentration (10, 14). Intercellular $CO_2$ concentration, in turn, varies with the rate of $CO_2$ supply through leaf stomata and the rate of $CO_2$ assimilatory demand. Since stomata respond to moisture conditions, $\Delta_{trc}$ correlations with humidity parameters are thought to derive from $CO_2$-supply-side effects on DR discrimination (6). By contrast, $CO_2$ assimilation responds to air temperature and solar radiation, and corresponding $\Delta_{trc}$ correlations are thought to derive form $CO_2$-demand-side effects on DR discrimination (6). Moreover, there is a mechanistic relationship between DR discrimination and *iWUE* (9, 10) which forms the basis of *iWUE* reconstructions from $\Delta_{trc}$ (6, 11). Note, all current $\Delta_{trc}$ interpretations assume that DR discrimination governs $\Delta_{trc}$ variation (6). Discrimination downstream of rubisco, denoted post-rubisco (PR) discrimination (12), is consider constant for any given species (11).

Recently, nuclear magnetic resonance spectroscopy was used (for the first time in dendrochronology) to measure intramolecular $^{13}C$ discrimination, $\Delta_i'$, in glucose extracted across a tree-ring series (*i* denotes glucose carbon position, C-1 to C-6) (12). This provided 6-fold higher resolution than (whole-molecule) $\Delta_{trc}$ analysis. The dataset was shown to contain multiple independent $^{13}C$ signals implying that DR discrimination is not the only variable component of $\Delta_{trc}$ (12). Follow-up studies elucidated signal properties and put forward theories on the signals' metabolic origins (see below, 13, 15, 16). Here, the relative contribution of intramolecular $^{13}C$ signals to $\Delta_{trc}$ were estimated by variance component analysis (*SI Appendix*, Supporting text T1). Furthermore, the capabilities of intramolecular versus whole-molecule carbon isotope analysis to investigate intramolecular $^{13}C$ signals were compared by multiple linear regression analysis. The results from these analyses form the basis for a critical reassessment of the classical concepts and practices of carbon-isotope dendrochronology and recommendations on the future research direction of the field.

**Intramolecular $^{13}C$ signals in *Pinus nigra* tree-ring glucose**

Previously, we measured intramolecular and whole-molecule $^{13}C$ discrimination of glucose ($\Delta_i'$ and $\Delta_{glu}$, respectively) across an annually resolved series of *Pinus nigra* tree rings (12). The dataset covers the period 1961 to 1995 but lacks measurements for 1977, 1978, 1981, and 1982 ($n$ = 31*6). $\Delta_i'$ was corrected for carbon redistribution by heterotrophic triose phosphate cycling (indicated by prime, 12). Results reported for tree-ring glucose ($\Delta_i'$ and $\Delta_{glu}$) presumably apply to tree-ring cellulose ($\Delta_{trc}$) because the former can be expected to largely derive from the latter.

We analysed $\Delta_1'$, $\Delta_2'$, and $\Delta_3'$ data pertaining to 1961 to 1980 (early period) and 1983 to 1995 (late period) separately, because the $\Delta_{1\text{-}2}'$ and $\Delta_{1\text{-}3}'$ series (denoting arithmetic averages of $\Delta_1'$ and $\Delta_2'$, and $\Delta_1'$ to $\Delta_3'$, respectively) exhibit a change point in 1980 (16). This change point was also found in $\Delta_{glu}$, and the variance of $\Delta_{glu}$ is four-fold higher during the late compared to the early period (1.47‰ versus 0.3‰, 16). Proposedly, the trees had access to groundwater during the early but not during the late period (17) causing metabolism affecting $\Delta_1'$ to $\Delta_3'$ to move from a largely homeostatic state into a climate-responsive state (16). By contrast, no change point was detected in $\Delta_4'$, $\Delta_5'$, and $\Delta_6'$ or average series thereof (16). Therefore, splitting these series was not required.

We (*inter alia*) used multiple linear regression modelling to find environmental and physiological covariates of $\Delta_i'$ (*SI Appendix*, Table S1) and proposed several ecophysiological mechanisms introducing the corresponding $\Delta_i'$ signals (*SI Appendix*, Fig. S1) (16). First, air vapour

 doi:10.20944/preprints202403.0014.v1



pressure deficit (*VPD*) was found to affect both $\Delta_1'$ and $\Delta_3'$ during the late period (Table 1, 16). This relationship is thought to derive from DR discrimination (in leaves). Additional $^{13}C$ discrimination by phosphoglucose isomerase (PGI) and/or glucose-6-phosphate dehydrogenase (G6PD) in leaves is thought to account for the stronger effect of *VPD* on $\Delta_1'$ compared to $\Delta_3'$. Second, during the late period, $\Delta_1'$ and $\Delta_2'$ are related to $\varepsilon_{met}$ denoting hydrogen isotope fractionation at glucose $H^1$ and $H^2$, and $\varepsilon_{met}$ can be substituted by precipitation without losing much of the models' explanatory power (16, 17). These relationships are thought to derive from $^{13}C$ discrimination by PGI and G6PD in tree stems (16). Note, the described $\Delta_1'$ to $\Delta_3'$ models do not work for the early period (16). Third, global radiation (*RAD*, data available from 1964) and air temperature (*TMP*) were found to affect $\Delta_4'$ to $\Delta_6'$ over the entire study period (16). These relationships are thought to derive from $^{13}C$ discrimination in leaves by glyceraldehyde-3-phosphate dehydrogenases (GAPDH) affecting $\Delta_4'$ and enzymes modifying the carbon double bond of phospho*enol*pyruvate affecting $\Delta_5'$ and $\Delta_6'$ (13, 15). For more comprehensive information about these mechanisms, the reader is referred to previous reports (12, 13, 15, 16, 18).

**Table 1.** Environmental and physiological covariates of $\Delta_i'$ and proposed enzymatic origins of corresponding $\Delta_i'$ signals.

| | | | Proposed origin of introduction | |
|---|---|---|---|---|
| **Covariate** | **Relationship** | **Period** | **Tissue** | **Enzyme** |
| $\Delta_1'$ ~ $\varepsilon_{met}$[(a)] | negative | 83 - 95 | Stem | PGI, G6PD |
| $\Delta_1'$ ~ ***VPD*** | negative | 83 - 95 | Leaf | PGI, G6PD, Rubisco[(b)] |
| $\Delta_2'$ ~ $\varepsilon_{met}$[(a)] | negative | 83 - 95 | Stem | PGI |
| $\Delta_3'$ ~ ***VPD*** | negative | 83 - 95 | Leaf | Rubisco[(b)] |
| $\Delta_4'$ ~ ***RAD*** | negative | 64 - 95 | Leaf | p-GAPDH, np-GAPDH |
| $\Delta_4'$ ~ ***TMP*** | positive | 64 - 95 | Leaf | |
| $\Delta_{5\text{-}6}'$ ~ ***RAD*** | negative | 64 - 95 | Leaf | PEPC, PK, DAHPS, Enolase |
| $\Delta_{5\text{-}6}'$ ~ ***TMP*** | positive | 64 - 95 | Leaf | |

Underlying models were published previously (*SI Appendix*, Models) (16). Proposed origins of $\Delta_i'$ signals in primary carbon metabolism are shown in *SI Appendix*, Fig. S1. $\varepsilon_{met}$, $\Delta_i'$, and $\Delta_{5\text{-}6}'$ denote hydrogen isotope fractionation by metabolic processes at glucose $H^1$ and $H^2$, carbon isotope discrimination at glucose carbon position, *i*, and the arithmetic average of $\Delta_5'$ and $\Delta_6'$, respectively. Glucose was extracted across an annually resolved tree-ring series of *Pinus nigra* from the Vienna Basin. Climate data series: *RAD*, April to September global radiation (data available from 1964); *TMP*, March to October air temperature; *VPD*, March to November air vapour pressure deficit. Enzymes: DAHPS, 3-Deoxy-D-*arabino*-heptulosonate-7-phosphate synthase; G6PD, glucose-6-phosphate dehydrogenase; np- and p-GAPDH, non-phosphorylating and phosphorylating glyceraldehyde-3-phosphate dehydrogenase; PEPC, phospho*enol*pyruvate carboxylase; PGI, phosphoglucose isomerase; PK, pyruvate kinase. [(a)] replacing $\varepsilon_{met}$ by March to July precipitation results in models with only slightly reduced explanatory power. [(b)] $^{13}C$ discrimination accompanying $CO_2$ diffusion and assimilation by rubisco is introduced into carbon metabolism at rubisco.

## Components of $\Delta_{glu}$ variation and implications for reconstructions of intrinsic water-use efficiency

Fig. 1 shows percent contributions of intramolecular isotope signals found by modelling (Tables 1 and S1) and model residuals to $\Delta_{glu}$ variation for the more dynamic late period (1983 to 1995, $n = 13$, $\Delta_{glu}$ variance = 1.47‰). Data of $\Delta_i'$ have significant measurement errors which largely account for the residuals of the $\Delta_1'$, $\Delta_3'$, $\Delta_4'$, and $\Delta_{5\text{-}6}'$ models (*SI Appendix*, Supporting text T2). By contrast, measurement errors account for only ≈30% of the residual variance of the $\Delta_2'$ model. Hence, this model may require extensions to capture the entire systematic variation of $\Delta_2'$. That said, the systematic $\Delta_2'$ variation not captured by modelling accounts for only ≈9% of the total $\Delta_{glu}$ variation

 doi:10.20944/preprints202403.0014.v1



(13.1*0.7, 16). Disregarding this component, leaf $^{13}C$ discrimination accounts for ≈43.5% of the total variance of $\Delta_{glu}$ while stem $^{13}C$ discrimination (related to $\varepsilon_{met}$) accounts for ≈19.5%. Furthermore, the contribution of leaf PR discrimination (≈25.9%) exceeds the contribution of leaf DR discrimination (≈8.8%*2 ≈ 17.6%). Hence, in contrast to its current practical treatment (11), PR discrimination is neither constant in leaves nor in stems.

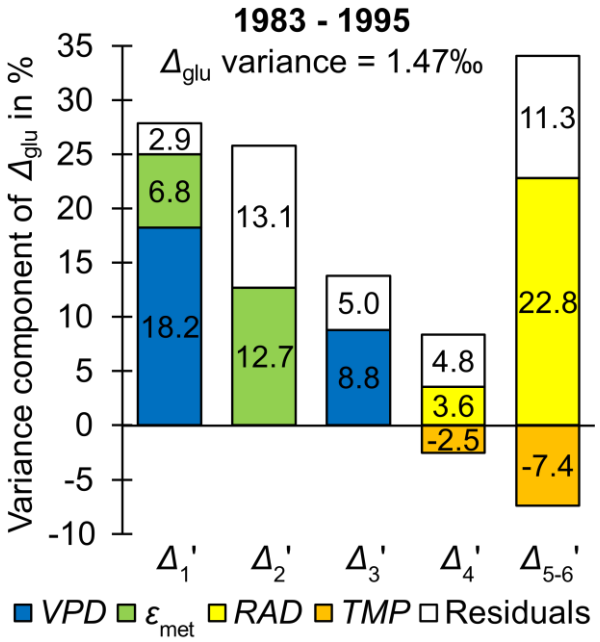


**Figure 1.** Percent contributions of intramolecular carbon isotope signals and model residuals to $\Delta_{glu}$ variation for the more variable late period (1980 to 1995, $n = 13$, $\Delta_{glu}$ variance = 1.47‰). Carbon isotope signals and model residuals were found by multiple regression modelling of $\Delta_i'$ as function of environmental and physiological covariates (16): *TMP*, March to October air temperature; *RAD*, April to September global radiation; *VPD*, March to November air vapour pressure deficit; $\varepsilon_{met}$, metabolic hydrogen isotope fractionation at glucose $H^1$ and $H^2$. $\Delta_i'$ denotes intramolecular $^{13}C$ discrimination where *i* denotes individual glucose carbon positions and the prime denotes data corrected for $^{13}C$ signal redistribution by heterotrophic triose phosphate cycling. $\Delta_{glu}$ denotes whole-glucose $^{13}C$ discrimination. Glucose was extracted across an annually resolved tree-ring series of *Pinus nigra* from the Vienna Basin.

*iWUE* is regarded as an important functional property of plant ecosystems and a key determinant in the response of regional and global carbon, water, and energy cycles to climate change (19, 20). Retrospective assessment of *iWUE* across large spatiotemporal scales relies on $\Delta_{trc}$ analysis (1–5) which, in turn, relies on the assumption that DR discrimination governs $\Delta_{trc}$ variability (6, 11, 21). However, DR discrimination accounts for merely ≈17.6% of the total variance of $\Delta_{glu}$ during the late period while PR discrimination accounts for ≈45.4% (Fig. 1). Hence, in the present case, $\Delta_{trc}$ should probably not be used as proxy of *iWUE* since the *iWUE* signal is strongly confounded by other signals. Since the *iWUE* signal is better resolved at the intramolecular level, $\Delta_i'$ analysis is expected to provide more accurate estimates of *iWUE*.

Findings presented for the late period are qualitatively consistent with findings pertaining to the early period (*SI Appendix*, Supporting text T3).

### Physiological interpretation of $\Delta_{trc}$-climate relationships

Depending on site characteristics (dry, moist, etc.), various climate parameters may govern $\Delta_{trc}$ variability ('Introduction', 6). That said, all reported $\Delta_{trc}$-climate relationships are currently interpreted with respect to DR discrimination.

 doi:10.20944/preprints202403.0014.v1



At the dry site discussed here, DR discrimination responds to *VPD* (16). However, while DR discrimination accounts for ≈17.6% of the total $\Delta_{glu}$ variance during the late period, *VPD*-dependent PR discrimination accounts for an additional ≈9.4% (Fig. 1). Hence, both DR and PR discrimination contribute to the *VPD* signal in $\Delta_{glu}$ and their combined contribution accounts for ≈27% of the total $\Delta_{glu}$ variance. Interestingly, linear regression between $\Delta_{glu}$ and *VPD* falsely suggests that *VPD* accounts for ≈54% of the total $\Delta_{glu}$ variance. This twofold overestimation of the *VPD* signal can be expected to result from intercorrelation of *VPD* with other climate parameters (e.g., Pearson correlation between *VPD* and *RAD*: $r = 0.6$, $p < 0.05$, $n = 13$).

More importantly, relationships of $\Delta_{glu}$ with *RAD* and *TMP* derive from leaf-level PR discrimination (13, 15, 16). Similarly, relationships of $\Delta_{glu}$ with $\varepsilon_{met}$ and *PRE* derive from stem-level PR discrimination (16). *RAD*-dependent PR discrimination accounts for ≈48.5% and ≈26.4% of the total $\Delta_{glu}$ variance during the early and late period, respectively, and exceeds the contribution of DR discrimination during both periods (Fig. 1; *SI Appendix*, Supporting text T3). Hence, most of the climate information in $\Delta_{glu}$ derives from PR discrimination and this can be expected to also apply to $\Delta_{trc}$.

**Detecting intramolecular isotope signals at the whole-molecule level**

It is highly interesting to ask whether intramolecular isotope analysis outperforms whole-molecule analysis or, more specifically, whether isotope signals detected in $\Delta_i'$ can also be found in $\Delta_{glu}$. To test this, $\Delta_{glu}$ data of the late period were modelled as function of *VPD*, $\varepsilon_{met}$, *RAD*, and *TMP* by multiple linear regression. Initially, potential interaction among independent variables was not considered. In the resulting model, $\Delta_{glu}$ is not significantly related with *VPD* and *TMP* (Table 2, M1). Subsequent models considered interaction among independent variables, and the model with the highest explanatory power is shown in Table 2 (M2). Again, in this model, $\Delta_{glu}$ is not significantly related with *TMP*. Hence, some isotope-climate relationships evident at the intramolecular level are invisible to whole-molecule analysis (*cf.* Tables 1 and S1, and Fig. 1). Additionally, whole-molecule analysis is blind to the intramolecular location of isotope signals and, therefore, offers no clues on the signals' metabolic origins. Thus, intramolecular isotope analysis exceeds the capabilities of whole-molecule analysis.

**Table 2.** Linear regression models of $\Delta_{glu}$ as function of $\varepsilon_{met}$, *VPD*, *RAD*, and *TMP*.

| **M1: $\Delta_{glu} \sim \varepsilon_{met} + VPD + RAD + TMP$, 1983-1995** | | | |
|---|---|---|---|
| $R^2 = 0.86$, $adjR^2 = 0.79$, $p < 0.002$, $n = 13$ | | | |
| | **Estimate** | **± SE** | ***p* ≤** |
| **Intercept** | 25.0 | 5.2 | 0.001 |
| $\varepsilon_{met}$ | -0.0142 | 0.0042 | 0.01 |
| ***VPD*** | -0.00753 | 0.00475 | 0.15 |
| ***RAD*** | -0.00475 | 0.00142 | 0.01 |
| ***TMP*** | 0.686 | 0.411 | 0.13 |
| **M2: $\Delta_{glu} \sim \varepsilon_{met} + VPD * RAD + TMP$, 1983-1995** | | | |
| $R^2 = 0.95$, $adjR^2 = 0.91$, $p < 0.0003$, $n = 13$ | | | |
| | **Estimate** | **± SE** | ***p* ≤** |
| **Intercept** | -21.7 | 14.2 | 0.2 |
| $\varepsilon_{met}$ | -0.0150 | 0.0028 | 0.001 |
| ***VPD*** | 0.0808 | 0.0263 | 0.02 |
| ***RAD*** | 0.0111 | 0.0048 | 0.05 |
| ***TMP*** | 0.347 | 0.289 | 0.27 |

 doi:10.20944/preprints202403.0014.v1



| | | | |
|---|---|---|---|
| ***VPD * RAD*** | -0.0000269 | 0.0000079 | 0.01 |

$\Delta_{glu}$ and $\varepsilon_{met}$ denote whole-molecule $^{13}C$ discrimination of glucose and average hydrogen isotope fractionation caused by metabolic processes at glucose $H^1$ and $H^2$, respectively. Glucose was extracted across an annually resolved tree-ring series of *Pinus nigra* from the Vienna Basin. Climate data series: *RAD*, April to September global radiation; *TMP*, March to October air temperature; *VPD*, March to November air vapour pressure deficit.

## Perspective

Here, recently reported results on the first dataset of intramolecular $^{13}C$ discrimination in tree rings were synthesised. The picture emerging from this synthesis is not in line with the classical (DR-discrimination-centred) concepts and practices of carbon-isotope dendrochronology and indicates that intramolecular carbon isotope analysis has a significant disruptive potential with respect to the scientific development of the field. It is important to note, however, that all currently proposed physiological interpretations of intramolecular $^{13}C$ signals require further testing and possibly revisions. Nevertheless, based on the large number of detected intramolecular $^{13}C$ signals (Fig. 1), the transition from whole-molecule to intramolecular carbon isotope analysis is expected to substantially enhance the amount and quality of information we can retrieve from tree rings. Furthermore, it is expected to substantially change how we interpretate and use tree-ring carbon isotope data.

Since disentangling intramolecular isotope signals by whole-molecule analysis cannot be achieved with sufficient confidence (Table 2), the field of carbon-isotope dendrochronology is strongly encouraged to enter the intramolecular level. Unfortunately, protocols using nuclear magnetic resonance spectroscopy to measure intramolecular $^{13}C$ discrimination are labour-intensive and require technology and know-how that is inaccessible to most dendrochronological laboratories. However, protocols enabling such measurements by Orbitrap mass spectrometry are currently under development (22, 23) and may soon facilitate the widespread use of intramolecular data in dendrochronology, paleoclimatology, biogeochemistry, and plant physiology. This exciting technological development will, in all probability, take our abilities to extract information archived in tree rings to the next level.

**Supplementary Materials:** The following supporting information can be downloaded at the website of this paper posted on Preprints.org.

**Data Availability Statement:** The author declares that the data supporting the findings of this study are available within the paper and its supporting information.

**Acknowledgements:** This work was carried out with funding from "Formas - a Swedish Research Council for Sustainable Development" (2022-02833, Grant recipient: TW).

**Conflicts of Interest:** None declared.

## References

1. M. Saurer, R. T. W. Siegwolf, F. H. Schweingruber, Carbon isotope discrimination indicates improving water-use efficiency of trees in northern Eurasia over the last 100 years. *Glob. Chang. Biol.* **10**, 2109–2120 (2004).
2. J. Peñuelas, J. G. Canadell, R. Ogaya, Increased water-use efficiency during the 20th century did not translate into enhanced tree growth. *GEB* **20**, 597–608 (2011).
3. D. C. Frank, *et al.*, Water-use efficiency and transpiration across European forests during the Anthropocene. *Nat. Clim. Change* **5**, 579–583 (2015).
4. P. van der Sleen, *et al.*, No growth stimulation of tropical trees by 150 years of $CO_2$ fertilization but water-use efficiency increased. *Nat. Geosci.* **8**, 24–28 (2015).

 doi:10.20944/preprints202403.0014.v1




5. M. A. Adams, T. N. Buckley, T. L. Turnbull, Diminishing $CO_2$-driven gains in water-use efficiency of global forests. *Nat. Clim. Change* **10**, 466–471 (2020).
6. M. Gagen, *et al.*, "Climate signals in stable isotope tree-ring records" in *Stable Isotopes in Tree Tings: Inferring Physiological, Climatic and Environmental Responses*, R. T. W. Siegwolf, J. R. Brooks, J. Roden, M. Saurer, Eds. (Springer International Publishing, 2022), pp. 537–579.
7. H. Craig, The geochemistry of the stable carbon isotopes. *GCA* **3**, 53–92 (1953).
8. H. Craig, Carbon-13 variations in Sequoia rings and the atmosphere. *Science* **119**, 141–143 (1954).
9. G. D. Farquhar, R. A. Richards, Isotopic composition of plant carbon correlates with water-use efficiency of wheat genotypes. *Aust. J. Plant Physiol.* **11**, 539–552 (1984).
10. G. D. Farquhar, M. H. O'Leary, J. A. Berry, On the relationship between carbon isotope discrimination and the intercellular carbon dioxide concentration in leaves. *Aust. J. Plant Physiol.* **9**, 121–137 (1982).
11. L. A. Cernusak, N. Ubierna, "Carbon isotope effects in relation to $CO_2$ assimilation by tree canopies" in *Stable Isotopes in Tree Rings: Inferring Physiological, Climatic and Environmental Responses*, R. T. W. Siegwolf, J. R. Brooks, J. Roden, M. Saurer, Eds. (Springer International Publishing, 2022), pp. 291–310.
12. T. Wieloch, *et al.*, Intramolecular $^{13}C$ analysis of tree rings provides multiple plant ecophysiology signals covering decades. *Sci. Rep.* **8**, 5048 (2018).
13. T. Wieloch, T. D. Sharkey, R. A. Werner, J. Schleucher, Intramolecular carbon isotope signals reflect metabolite allocation in plants. *J. Exp. Bot.* **73**, 2558–2575 (2022).
14. J. R. Evans, G. D. Farquhar, T. D. Sharkey, J. A. Berry, Carbon isotope discrimination measured concurrently with gas exchange to investigate $CO_2$ diffusion in leaves of higher plants. *Aust. J. Plant Physiol.* **13**, 281–292 (1986).
15. T. Wieloch, R. A. Werner, J. Schleucher, Carbon flux around leaf-cytosolic glyceraldehyde-3-phosphate dehydrogenase introduces a $^{13}C$ signal in plant glucose. *J. Exp. Bot.* **72**, 7136–7144 (2021).
16. T. Wieloch, M. Holloway-Phillips, J. Yu, T. Niittylä, New insights into the mechanisms of post-rubisco isotope fractionation from combined analysis of intramolecular $^{13}C$ and deuterium abundances in *Pinus nigra* tree-ring glucose. *bioRxiv*, 2024.02.21.581384 (2024). Submitted to *New Phyt.* on the 12th of January 2024.
17. T. Wieloch, *et al.*, Metabolism is a major driver of hydrogen isotope fractionation recorded in tree-ring glucose of *Pinus nigra*. *New Phytol.* **234**, 449–461 (2022).
18. T. Wieloch, A cytosolic oxidation–reduction cycle in plant leaves. *J. Exp. Bot.* **72**, 4186–4189 (2021).
19. T. F. Keenan, *et al.*, Increase in forest water-use efficiency as atmospheric carbon dioxide concentrations rise. *Nature* **499**, 324–327 (2013).
20. C. Beer, *et al.*, Temporal and among-site variability of inherent water use efficiency at the ecosystem level. *Glob. Biogeochem. Cycles* **23** (2009).
21. W. T. Ma, Y. Z. Yu, X. Wang, X. Y. Gong, Estimation of intrinsic water-use efficiency from $\delta^{13}C$ signature of $C_3$ leaves: Assumptions and uncertainty. *Front. Plant Sci.* **13** (2023).
22. C. Neubauer, *et al.*, Discovering nature's fingerprints: Isotope ratio analysis on bioanalytical mass spectrometers. *J. Am. Soc. Mass Spectrom.* **34**, 525–537 (2023).
23. E. B. Wilkes, *et al.*, Position-specific carbon isotope analysis of serine by gas chromatography/Orbitrap mass spectrometry, and an application to plant metabolism. *Rapid Commun. Mass Spectrom.* **36**, e9347 (2022).